Available online at www.sciencedirect.com

ScienceDirect

Remote Sensing of Environment 112 (2008) 2160–2169

Remote Sensing of Environment

www.elsevier.com/locate/rse

# Evaluating MODIS data for mapping wildlife habitat distribution

Andrés Viña [a,*], Scott Bearer [a,1], Hemin Zhang [b], Zhiyun Ouyang [c], Jianguo Liu [a]

[a] *Center for Systems Integration and Sustainability, Department of Fisheries and Wildlife, Michigan State University, East Lansing, MI, USA*
[b] *China's Center for Giant Panda Research and Conservation, Wolong Nature Reserve, Sichuan, China*
[c] *State Key Lab of Urban and Regional Ecology, Research Center for Eco-Environmental Sciences, Chinese Academy of Sciences, Beijing, China*

Received 24 October 2006; received in revised form 30 July 2007; accepted 14 September 2007

**Abstract**

Habitat distribution models have a long history in ecological research. With the development of geospatial information technology, including remote sensing, these models are now applied to an ever-increasing number of species, particularly those located in areas in which it is logistically difficult to collect habitat data in the field. Many habitat studies have used data acquired by multi-spectral sensor systems such as the Landsat Thematic Mapper (TM), due mostly to their availability and relatively high spatial resolution (30 m/pixel). The use of data collected by other sensor systems with lower spatial resolutions but high frequency of acquisitions has largely been neglected, due to the perception that such low spatial resolution data are too coarse for habitat mapping. In this study we compare two models using data from different satellite sensor systems for mapping the spatial distribution of giant panda habitat in Wolong Nature Reserve, China. The first one is a four-category scheme model based on combining forest cover (derived from a digital land cover classification of Landsat TM imagery acquired in June, 2001) with information on elevation and slope (derived from a digital elevation model obtained from topographic maps of the study area). The second model is based on the Ecological Niche Factor Analysis (ENFA) of a time series of weekly composites of WDRVI (Wide Dynamic Range Vegetation Index) images derived from MODIS (Moderate Resolution Imaging Spectroradiometer – 250 m/pixel) for 2001. A series of field plots was established in the reserve during the summer–autumn months of 2001–2003. The locations of the plots with panda feces were used to calibrate the ENFA model and to validate the results of both models. Results showed that the model using the seasonal variability of MODIS-WDRVI had a similar prediction success to that using Landsat TM and digital elevation model data, albeit having a coarser spatial resolution. This suggests that the phenological characterization of the land surface provides an appropriate environmental predictor for giant panda habitat mapping. Therefore, the information contained in remotely sensed data acquired with low spatial resolution but high frequency of acquisitions has considerable potential for mapping the habitat distribution of wildlife species.


*Keywords:* Giant panda; Habitat distribution models; Landsat Thematic Mapper (TM); Moderate Resolution Imaging Spectroradiometer (MODIS); Wide Dynamic Range Vegetation Index (WDRVI); Wolong Nature Reserve (China)

## 1. Introduction

Deciding which areas are the most important for conservation and management requires a precise knowledge of the locations and spatial distribution of target species habitats (Rushton et al., 2004). This is particularly important for both invasive (Peterson, 2005; Morisette et al., 2006) and endangered (Engler et al., 2004; Xu et al., 2006) species for which such knowledge can be used to establish strategies for managing their population dynamics (Rushton et al., 2004). It is also important when the habitat of the target species for conservation encompasses the habitat of numerous other plant and animal species (e.g., flagship species), therefore establishing management efforts that embrace entire ecosystems. Such is the case of the endangered giant panda (*Ailuropoda melanoleuca*), which not only is a global icon for biodiversity conservation, but its habitat comprises several types of sub-alpine forest ecosystems (Reid & Hu, 1991; Taylor & Qin, 1993). Therefore, efforts to mitigate the habitat reduction of this conservation icon can also promote the conservation of entire forest ecosystems.

* Corresponding author. Center for Systems Integration and Sustainability, 1405 S. Harrison Road, Suite 115 Mainly Miles Bldg., Michigan State University, East Lansing, MI 48823-5243, USA. Tel.: +1 517 432 5078.
*E-mail address:* vina@msu.edu (A. Viña).
[1] Current address: The Nature Conservancy, Williamsport, PA, USA.

0034-4257/$ - see front matter © 2008 Elsevier Inc. All rights reserved.
doi:10.1016/j.rse.2007.09.012

The giant panda once ranged throughout most of eastern and southern China, northern Vietnam, and northern Myanmar (Pan et al., 2001), but it has been restricted in recent decades to six major mountainous areas in China (Reid & Gong, 1999; Loucks et al., 2001). The main reasons for the reduction in its geographic range are the human-induced loss and fragmentation of broadleaf deciduous and coniferous montane forests, as the pandas rely on forest overstory as shelter and understory bamboo as staple food (Schaller et al., 1985; Taylor & Qin, 1987, 1993; Reid & Hu, 1991; Reid et al., 1991; Liu et al., 1999). Conservation of this species constitutes an enormous challenge and a national priority for China, since there are only about 1600 individuals in the wild (Wei et al., 2006), distributed in approximately 24 isolated populations across its current estimated geographic range (Reid & Gong, 1999; Loucks et al., 2001; Yan, 2005).

The increasing availability of remotely sensed data acquired by operational satellites, coupled with the development of geographic information systems (GIS) capable of storing and analyzing the enormous amounts of spatial data generated by remote sensing techniques, has led to their widespread use in habitat mapping (Rushton et al., 2004). The common approach employed for habitat mapping using remotely sensed data has been the generation of non-hierarchical land cover classifications, combined with ancillary information such as digital elevation models (DEM) derived from topographic maps (e.g., Luoto et al., 2002a,b). Most of these exercises have favored remotely sensed data acquired at spatial resolutions similar to field observations (e.g., 30×30 m field plots; Seto et al., 2004), with Landsat Thematic Mapper (TM) data being the most highly used, primarily due to their availability. Giant panda habitat mapping has not escaped this trend since it has primarily relied on land cover classifications of Landsat imagery using visual interpretations (MacKinnon & De Wulf, 1994; Liu et al., 2001), as well as digital image processing techniques such as unsupervised (Loucks et al., 2003; Viña et al., 2007) and supervised (Xu et al., 2006) procedures. However, these techniques have not been able to detect the spectral signature of understory bamboo cover. That is important for characterizing the panda habitat (Linderman et al., 2004), since the optical response of the vegetation captured by the satellite sensor is a complex non-linear combination of overstory and understory canopy components (Borel & Gerstl, 1994). Therefore, other digital processing techniques based on neural networks have been proposed in order to detect the presence of understory bamboo in Landsat imagery (Linderman et al., 2004; Liu et al., 2004), and have been shown to modify the areal estimates of panda habitat (Linderman et al., 2005).

Furthermore, due to the low temporal resolution of Landsat imagery, the data used in habitat analyses usually correspond to snapshots at particular dates and seasons that fail to recognize the seasonal nature of habitats (Nielsen et al., 2003). Although some studies have acknowledged that multi-temporal data enable the classification of seasonally changing habitats, and have used two or more Landsat scenes acquired during different seasons (e.g., Luoto et al., 2002a,b), the phenological progression of the vegetation has not been fully evaluated for habitat characterization and mapping.

High temporal resolution data, such as the widely available global datasets derived from the Advanced Very High Resolution Radiometer (AVHRR) or the Moderate Resolution Imaging Spectroradiometer (MODIS), can be used to evaluate the phenological progression of the vegetation, and potentially constitute suitable environmental predictors for habitat mapping (Morisette et al., 2006). Nevertheless, the use of these data for habitat mapping has been largely neglected due mostly to their coarse spatial resolutions (250 m–1 km/pixel).

The main goal of this study is to evaluate the usefulness of MODIS time series imagery, as compared to the traditional classification of single-date Landsat TM imagery, for mapping the habitat for the endangered giant pandas. The rationale for this comparison is to examine whether data acquired with a high temporal resolution (as that of MODIS), although acquired with coarser spatial resolutions, can also be successfully used for mapping wildlife habitat. In addition, in order to implement comprehensive sustainable management practices for the conservation of the species such as establishment of nature reserves, buffer areas, corridors and re-introduction sites, it is important to analyze the distribution of existing panda habitat in its entire geographic range. Therefore, an important consideration for the usefulness of MODIS, as opposed to Landsat data, is their coverage of vast areas (regional to global extents), suitable for analyzing the habitat distribution of the entire geographic range of the species.

## 2. Methods

### 2.1. Study area

Wolong Nature Reserve is located in Sichuan Province, southwest China (Fig. 1). It was initially established in 1963 with an area of about 200 km$^2$ and then expanded to its current size of ca. 2000 km$^2$ in 1975 (Li et al., 2003). It is one of the largest nature reserves in China designed to protect the endangered giant pandas. Wolong Nature Reserve is part of the international Man and the Biosphere Reserve Network (He et al., 1996), protects approximately 10% of the entire wild panda population (Zhang et al., 1997), and has drawn unmatched domestic and international attention (Liu et al., 1999).

Situated the transition between the Sichuan Basin and the Qinghai-Tibet Plateau, it is characterized by high mountains and deep valleys, with elevations between 1200 m and 6250 m (Fig. 1). Together with this strong altitudinal gradient there is a high variation in topography, soils and climate that leads to a diverse flora and fauna. Vegetation in the reserve is dominated by evergreen and deciduous broadleaf forests at lower elevations (around 1500 m) and sub-alpine coniferous forests at higher elevations (around 2700 m; Schaller et al., 1985), with a dense understory dominated by bamboo species such as *Bashania fabri* and *Fargesia robusta* that are the staple food of the giant pandas in the reserve (Schaller et al., 1985; Taylor & Qin, 1987, 1993; Reid & Hu, 1991; Reid et al., 1991).

### 2.2. Giant panda occurrence

Being a bashful species, with only around 1600 individuals left in the wild (Wei et al., 2006) and a large distribution range, the endangered giant pandas are extremely difficult to encounter

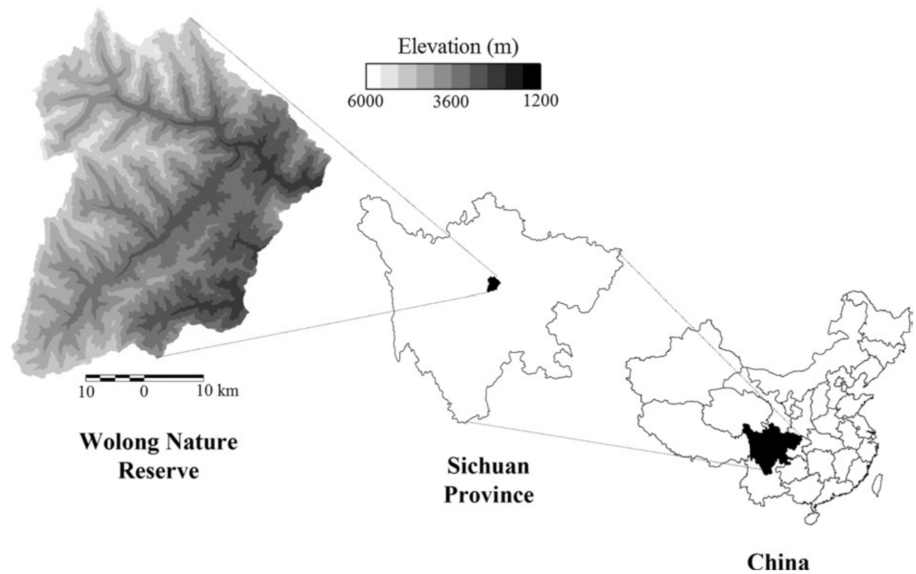


Fig. 1. Location of the Wolong Nature Reserve in Sichuan Province, China. Elevation is represented in shades of gray.

in the wild. Therefore, the spatial distribution of their fecal droppings was used as a surrogate of the species occurrence. Fecal droppings are a straightforward indicator of the occurrence of the species because they are deposited frequently (an average of 4 droppings/h) and remain visible for several months (Schaller et al., 1985).

A total of 443 field sampling plots (30 × 30 m) were located throughout Wolong Nature Reserve. Sampling plot location was randomly established before the field campaigns, although several of these previously established locations were rejected in the field due to access difficulties. Each of these plots was visited one time during one of three field campaigns in May–August 2001, May–November 2002, and June–August 2003 (Bearer, 2005). The center of each sampling plot was geo-referenced using a real-time differentially corrected Global Positioning System (GPS) receiver. Panda fecal droppings' presence, as well as the number of droppings, was determined in each plot. Seventy one field sampling plots, or 16%, exhibited panda fecal droppings (Bearer, 2005).

### 2.3. Landsat data

This study used cloud-free multi-spectral Landsat 5 Thematic Mapper (TM) images (WRS-2 Path 130, Rows 38-39) acquired on June 13, 2001 and obtained from the China Remote Sensing Satellite Ground Station. These images were radiometrically rectified by means of standard procedures (Markham & Barker, 1986) and geo-referenced to the WGS84 UTM coordinate system using the nearest neighbor algorithm (Jensen, 1996). A map of forest/non-forest in the reserve was obtained from this imagery, via a nested unsupervised classification algorithm, with an accuracy of ca. 80% (Viña et al., 2007). This algorithm involves a preliminary unsupervised classification that sorts the multi-spectral data into several spectral classes. These spectral classes are then assigned to land cover classes using ground-truth field data. Pixels in spectral classes that cannot be accurately assigned to a land cover class are isolated, and a successive unsupervised classification of the multi-spectral data is then applied only to these non-assigned pixels. This algorithm was particularly useful to extract land cover information on topographically shaded areas. Details of the procedure are given in Viña et al. (2007).

### 2.4. Moderate Resolution Imaging Spectroradiometer (MODIS) data

The MODIS/Terra surface reflectance 8-day L3 250m global product (MOD09Q1) was used in this study. This standard product is a composite of the previous 8 daily L2G surface reflectance products (MOD09GQK). This product has surface reflectance values of two spectral bands acquired with a spatial resolution of 250 m/pixel: red (620–670 nm) and near infrared (841–876 nm). Data acquired between January and December of 2001 (a total of 45 images) was obtained from the National Aeronautics and Space Administration (NASA) Earth Observation System (EOS) Data Gateway. The MODIS 8-day surface reflectance data were used to calculate a new vegetation index that is non-linearly related to the widely used Normalized Difference Vegetation Index (NDVI) (Rouse et al., 1974), called the Wide Dynamic Range Vegetation Index (WDRVI) (Gitelson, 2004):

$$\mathrm{WDRVI} = [(\alpha+1)\mathrm{NDVI} + (\alpha-1)]/[(\alpha-1)\mathrm{NDVI} + (\alpha+1)] \tag{1}$$

The weighting coefficient $\alpha$ downweights the contribution of the near infrared band in the NDVI formulation, making it comparable to that of the red band (Gitelson, 2004). Following the approach proposed by Henebry et al. (2004), an $\alpha = 0.25$ was selected as the optimum for the MODIS time series dataset used in the study.

Although the NDVI has been used extensively as a surrogate for vegetation biophysical characteristics such as the fraction of absorbed photosynthetically active radiation (*f*APAR; Asrar et al., 1992; Sellers, 1985) or the leaf area index (LAI; Myneni et al., 1997), it loses sensitivity at *f*APAR > 0.7 (Goward & Huemmerich, 1992; Viña & Gitelson, 2005) or LAI > 2 (Myneni et al., 1997; Gitelson et al., 2003). This sensitivity loss conceals the spatio-temporal variability of vegetation with moderate-to-high green biomass (Viña et al., 2004), such as the forest canopies with a dense understory present in the study area. Although other vegetation indices have been proposed to correct for this sensitivity loss (Enhanced Vegetation Index, Huete et al., 1997; Chlorophyll indices, Gitelson et al., 2005), they require additional spectral bands. Thus, the WDRVI was selected in this study because it constitutes a non-linear function of the NDVI, therefore suitable to be used with the 250 m/pixel near infrared and red spectral bands of the MODIS sensor. The WDRVI has been shown to be linearly related to the *f*APAR of crop canopies (Viña & Gitelson, 2005).

Due to the extensive cloud cover observed in the study area, with some pixels being continuously obscured by clouds for long periods of time (e.g., more than 3 weeks), it was necessary to apply an algorithm for the removal of cloud contaminated data from the 2001 time series of MODIS-WDRVI imagery. For this, the Harmonic Analysis of Time Series (HANTS) algorithm (Roerink et al., 2000) was used. This algorithm was designed to remove cloud contaminated pixel data from a time series of imagery, and replace it with interpolated data obtained through a weighted least squares curve fitting process based on harmonic sines and cosines established in the frequency domain (Verhoef et al., 1996). The algorithm runs an iterative process in which the observed values are compared to the curve values. If an observed value is significantly different from the predicted by the curve, it is eliminated and a new curve is computed using the remaining values. The curve fitting is, therefore, based only on cloud-free samples (Roerink et al., 2000).

Five controlling parameters are required to be specified in advance in order to run the HANTS algorithm (Roerink et al., 2000): (1) Frequency numbers, which determine how many oscillations are going to be used and the extent of their corresponding period in time sample units. This parameter consists of the zero frequency (the average pixel value of the cloud-free samples), the base frequency (length of the entire time series) and the overtones (multiples of the base frequency). In this study, the base frequency was 12 months, while 3 and 6 months where the overtones used, to account for the green-up and senescence periods, as well as the seasonal variations of the vegetation. (2) Hi/Lo suppression flag (SF), which indicates whether high or low values (outliers) should be rejected during the curve fitting. In this study low WDRVI values were rejected because cloud contamination always produces low WDRVI values. (3) Invalid data rejection threshold (IDRT), which establishes the range of variation within which the data are considered to be valid. A range between −0.7 and 0.6 (in WDRVI units) was chosen, corresponding to the minimum and maximum values observed in the time series dataset, which includes the WDRVI values of snow and ice occurring at high elevations. (4) Fitting error tolerance (FET), which represents the maximum acceptable absolute deviation in the chosen direction of the Hi/Lo suppression flag, therefore determining when the iterative curve fitting process should stop. A high value will cause the algorithm to remove few invalid values, thus leaving many cloud contaminated pixels, while a low value will lead to the removal of many observed values. A value of 0.05 (in WDRVI units) was assigned in this study as the fitting error tolerance. (5) Degree of overdeterminedness (DOD), which represents the minimum number of data points that are required in the ultimate curve fit. Since the number of valid observations must always be at least equal to the number of parameters that describes the curve, the use of more data points than the necessary minimum will produce a more reliable fit. A DOD value of 13 was used.

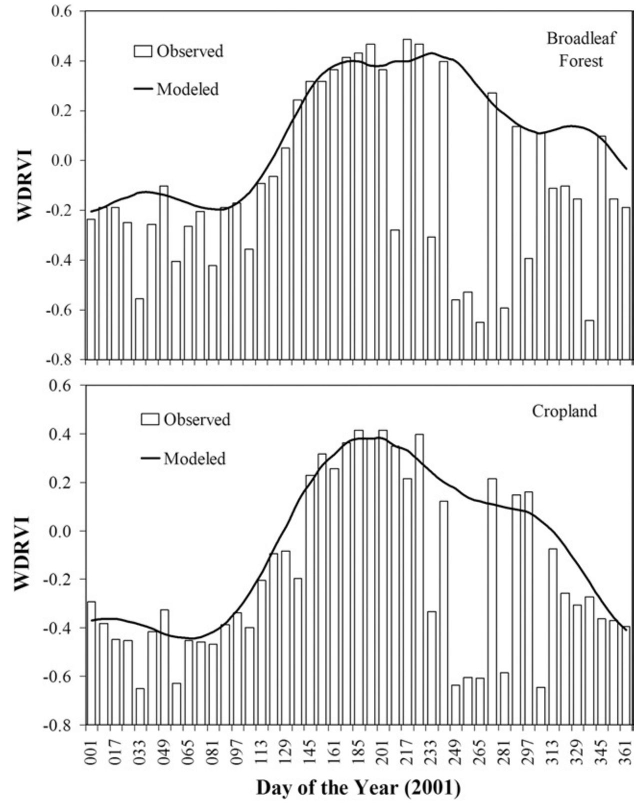


Fig. 2. Comparison of the observed and modeled cloud-free MODIS-WDRVI 2001 time series in two pixels under different land cover types (deciduous forest and cropland). This figure demonstrates the ability of the HANTS algorithm for generating cloud-free time series imagery.

One of the disadvantages of the HANTS algorithm is that there are no objective rules to determine these control parameters (Roerink et al., 2000). Therefore, the parameters used in this study were selected after running the HANTS algorithm with different parameter combinations and establishing the best fit, which is the lowest root mean squared error between a cloud-free observed sample and its modeled value, on randomly selected pixels. Fig. 2 shows the comparison of observed and modeled 2001 MODIS-WDRVI time series for two pixels classified as (a) broadleaf deciduous forest, and (b) cropland. Fig. 3 shows the spatial distribution of observed and modeled MODIS-WDRVI values in Wolong Nature Reserve during a period of widespread cloud cover. These figures show that the HANTS algorithm is able to reconstruct a cloud-free time series of MODIS-WDRVI to be used for panda habitat mapping.

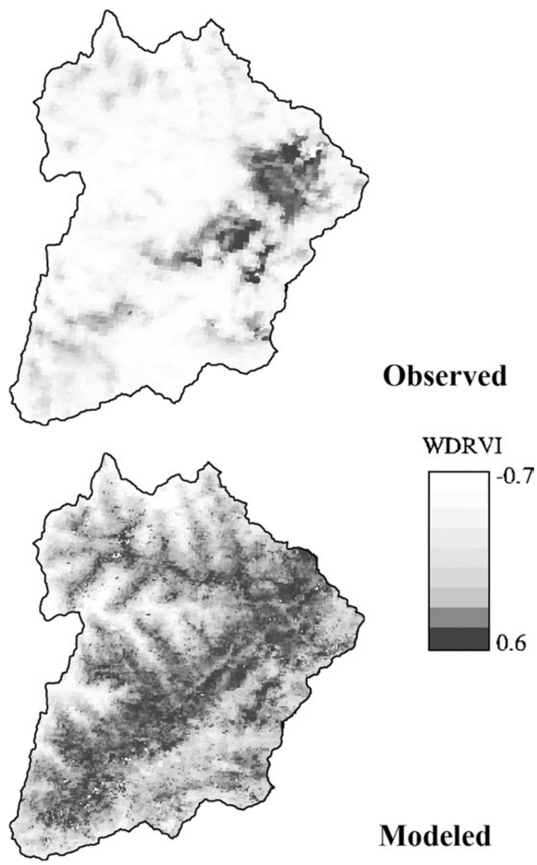


Fig. 3. Comparison of the MODIS-WDRVI 8-day composite image acquired on August 29 to September 5 (days of the year 241 to 248), which exhibited an extensive cloud cover in almost the entire nature reserve, and its modeled (cloud-free) MODIS-WDRVI 8-day composite image obtained using the HANTS algorithm.

### 2.5. Giant panda habitat distribution modeling

Two models for establishing the distribution of giant panda habitat using different satellite imagery were produced and compared. The first one is a four-category scheme model (Liu et al., 1999) based on the combination of three of the main biological requirements of the species (Schaller et al., 1985; Johnson et al., 1988; Reid et al., 1989; Ouyang et al., 1995): (1) areas under forest cover; (2) altitudinal range between 1500 and 3750 m, with an optimal range between 2250 and 2750 m; and (3) slopes of less than 45°, with optimal slopes of less than 15°. Information on forest cover was obtained from a nested unsupervised digital classification algorithm applied to the Landsat TM imagery acquired on June 13, 2001 (Viña et al., 2007), while information on elevation and slope were derived from a 30 m/pixel digital elevation model (DEM) developed from 1:50,000 topographic maps of the study area (Liu et al., 2001). The output of this combination is a habitat suitability map divided into four categories (Liu et al., 2001): highly suitable, moderately suitable, marginally suitable and unsuitable.

The second model was based on the ecological niche concept in which a species can be quantitatively represented in terms of a multidimensional combination of abiotic and biotic variables required for a viable population to persist (Hutchinson, 1957). Several habitat distribution models are based on this concept, many of which rely on presence/absence data. Because this study uses the spatial location of fecal droppings to determine the occurrence of the giant panda, instead of actual observations of the species, the lack of fecal droppings in a particular sampling plot does not necessarily imply that it constitutes an area of unsuitable habitat. Therefore, a model based on presence/availability data is preferred. Such models assume that the locations where the species of interest is observed are drawn from a sample of available sites, thus, the observed values must be a subset of what is available (Boyce et al., 2002). One of such models was used in this study, the Ecological Niche Factor Analysis (ENFA) developed by Perrin (1984) and implemented in the software Biomapper (Hirzel et al., 2002, 2004).

The ENFA compares the distribution of environmental variables of the study area against the distribution of the same variables in the species occurrence dataset (i.e., the locations within the study area where the species was observed), each stored as a raster layer in a GIS. In this study, the geographic locations of the 71 field plots with panda fecal droppings (converted to a raster format that matched the grain and extent of the MODIS imagery) were employed in the ENFA, together with the 2001 time series (45 images) of 250 m/pixel MODIS-WDRVI imagery used as an environmental predictor of giant panda habitat.

The ENFA summarizes the environmental predictor variables into a few orthogonal factors that retain most of the variance present in the multidimensional space. The first factor is established so that it passes through the centroid of the multidimensional species occurrence dataset and the centroid of the entire (or global) multidimensional dataset within the study area. This factor represents how different the environmental requirements of the species are from the average environmental conditions of the entire study area (Hirzel et al., 2002). Successive orthogonal factors are then calculated in order to maximize the ratio between the variance of the entire (or global) dataset within the study area and the variance of the species occurrence dataset. A high value of this ratio indicates that the species has a restricted environmental tolerance compared with the overall range of variability observed in the study area (Hirzel et al., 2002).

A map with the distribution of panda habitat suitability index (HSI) values (ranging from 0 to 100) was then obtained by using the geometric mean algorithm (Hirzel & Arlettaz, 2003). This algorithm computes, in the factorial space, the geometric mean of all the distances between each pixel of the global dataset to all the species observations (species dataset). This procedure was preferred because it does not assume any distribution of the species occurrence plots, therefore it is robust when the species occurrence data have asymmetrical, non-Gaussian, bi- or multi-modal distributions (Hirzel & Arlettaz, 2003). In addition, this procedure attained the highest prediction success (see model validation procedures below) among the algorithms tested (i.e., minimum distance, median and harmonic mean; Hirzel et al., 2004).

### 2.6. Model validation

Validation of the giant panda habitat maps produced with the two models could not be accomplished using traditional methods based on contingency tables (e.g., user/producer errors, Kappa coefficient, Receiver Operating Characteristic – ROC plots),

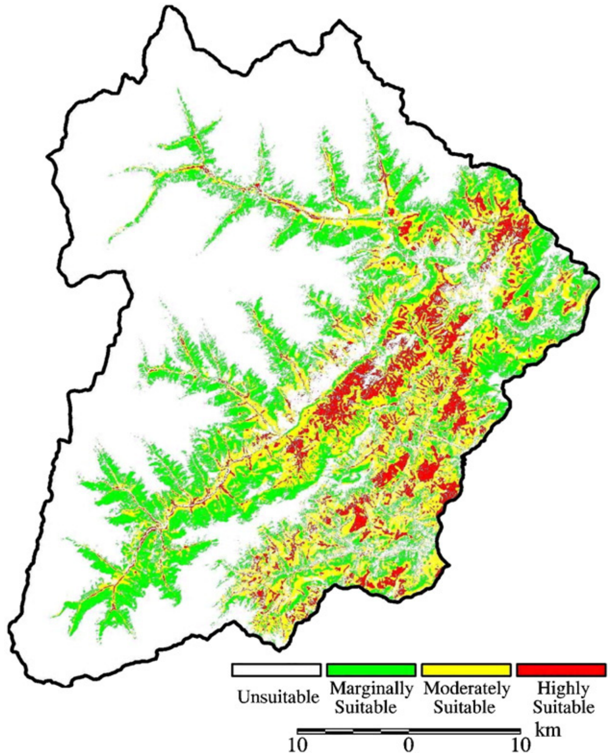


Fig. 4. Giant panda habitat distribution across Wolong Nature Reserve in 2001, based on the combination of forest cover (derived from Landsat TM data acquired in June 13, 2001), elevation and slope (derived from a digital elevation model).

because no field validation information was available for evaluating the species absences. Therefore, a different approach developed by Boyce et al. (2002) was used in order to validate the habitat suitability maps using presence-only data. For this, an area-adjusted frequency of validation plots is obtained for each habitat suitability class. This area-adjusted frequency corresponds to the frequency of field validation plots that fall in each class, divided by the frequency of locations (i.e., pixels) belonging to the same class across the study area. An area-adjusted frequency of 1.0 indicates that the validation plots occur at rates expected by chance (Boyce et al., 2002). A Spearman-rank correlation coefficient (Rs) is then calculated between the area-adjusted frequency of validation plots in each habitat suitability class and the habitat suitability class rank. A model with high predictive success should have high Rs, as more observed giant panda occurrences (i.e., plots with feces) would continually fall within higher habitat suitability class ranks (Boyce et al., 2002).

In the case of the first model, we utilized all the 71 field sampling plots that exhibited panda fecal droppings as validation plots. In the case of the second model, since we also used the same field plots to calibrate and validate the ENFA, we used a *k*-fold cross-validation procedure in which the panda occurrence data were iteratively divided into five cross-validation groups following a *k*-fold partitioning design. In this design, data are split into $k (k > 2)$ sets, one of which is used iteratively for validation and the remaining $k-1$ sets are pooled for calibration, thus making the accuracy estimate less dependent on a single partition (Fielding & Bell, 1997). The habitat suitability index (HSI) maps obtained in all iterations were sorted into four bins: 0–24.9, 25–49.9, 50–74.9 and 75–100, and the area-adjusted frequency of cross-validation occurrences was calculated for each of the HSI bins. This procedure was repeated 20 times using different *k*-fold partitions in order to obtain a distribution of validation results.

It is important to mention that this validation technique is particularly useful for comparing habitat maps obtained using different models but does not provide an absolute estimation of classification accuracy. Knowledge of the true absences would be required for such absolute accuracy estimation. Therefore, to provide context to the validation results, the model's performance was compared against that of a null model. The simplest null model is a random map in which all factors that might structure the spatial patterns are lacking (Gardner et al., 1987). A random map was developed using ENFA and the 2001 time series of 250 m/pixel MODIS-WDRVI imagery together with the geographic locations of 300 occurrence plots randomly located throughout Wolong Nature Reserve. Under this null model any pixel within the study area has the same probability of being panda habitat.

### 2.7. Panda habitat areal estimate comparison among models

In order to compare the total areal estimates of the panda habitat in Wolong Nature Reserve obtained with the ENFA model and with the four-category scheme model using Landsat TM data and a DEM, a threshold value was obtained for converting the continuous scale of the ENFA HSI into a binary decision of habitat and non-habitat areas. The criterion for threshold selection was based on a parsimony rule in which a good habitat suitability map obtained from presence-only data should predict the smallest habitat area as possible, but that still encompasses the maximum number of observed species occurrences (Engler et al., 2004). Using this rule, pixels with HSI of $>15$ were classified as panda habitat, since with this threshold the total area considered as panda habitat encompassed no less than 80% of the field plots with panda fecal droppings.

## 3. Results

### 3.1. Four-category scheme model using Landsat TM data and a DEM

The four-category habitat suitability map obtained from combining forest cover (derived from Landsat TM data), elevation and slope (derived from a DEM) is shown on Fig. 4. Total giant panda habitat obtained with this model (combining highly suitable, moderately suitable and marginally suitable) corresponds to 719.5 $km^2$, which accounts for 36% of the entire nature reserve. The results of the validation of this model are shown in Fig. 5. A high prediction success ($Rs = 0.92$) was obtained with this model.

### 3.2. ENFA model using MODIS-WDRVI 2001 time series data

The spatial distribution of panda habitat suitability index (HSI) values obtained from the ENFA model using the 2001

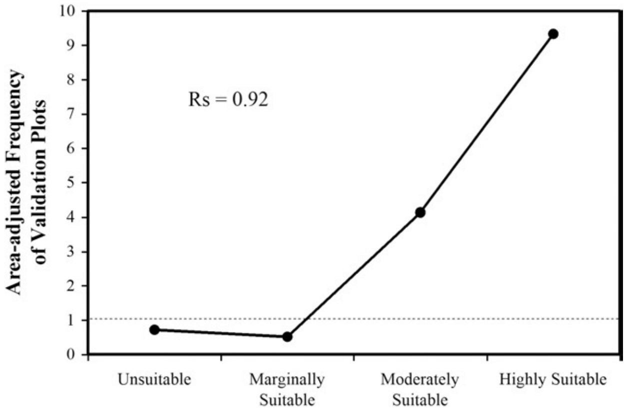


Fig. 5. Area-adjusted frequency of validation plots for each of the habitat suitability classes obtained using the Landsat TM imagery acquired on June 13, 2001 and a digital elevation model. Rs corresponds to the Spearman-rank correlation coefficient. Area-adjusted frequency values that are smaller than one indicate avoidance, while those that are greater than one indicate preference. Values closer to one (dotted line) indicate that the observed frequencies are not different from the random expectation.

time series of MODIS-WDRVI images is shown in Fig. 6. Validation of this model is shown in Fig. 7. As shown in this figure, the model performed significantly better than a random model and its prediction success (Rs) was similar to that obtained by the four-category scheme model using a DEM and Landsat TM data with a higher spatial resolution (Fig. 5). Considering that pixels with a HSI of >15 were classified as panda habitat (parsimony rule), the total average panda habitat

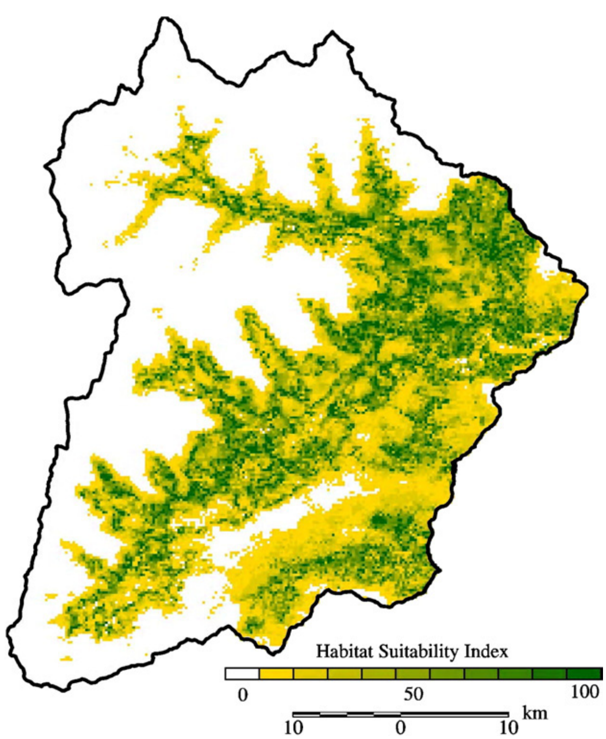


Fig. 6. Spatial distribution of giant panda habitat suitability index (HSI) values across Wolong Nature Reserve. The map was derived from an Ecological Niche Factor Analysis (ENFA) applied to a 2001 time series of Wide-dynamic Range Vegetation Index (WDRVI) images obtained from the Moderate Resolution Imaging Spectroradiometer (MODIS).

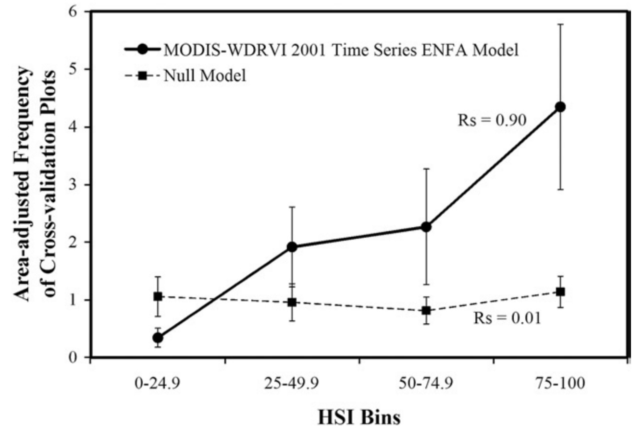


Fig. 7. Area-adjusted frequency of cross-validation plots for each of the four habitat suitability index (HSI) bins obtained in the ENFA model using the MODIS-WDRVI 2001 time series data and in the null model (i.e., random map). The area-adjusted frequency values that are smaller than one indicate avoidance, while those that are greater than one indicate preference. Values closer to one indicate that the observed frequency is not different from the random expectation. The symbols represent average values and the bars represent the standard deviations. Rs corresponds to the average Spearman-rank correlation coefficient.

area obtained corresponds to 710.8 km$^2$, with a standard deviation of 25.8 km$^2$. This accounts for around 35.5% of the entire nature reserve and is similar to that obtained by the model using Landsat TM data and a DEM. These results show that the information contained in the high temporal resolution MODIS data can be used as a suitable environmental predictor of panda habitat, despite its coarser spatial resolution.

## 4. Discussion

Mapping the habitat for the giant pandas using single-date multi-spectral remotely sensed data has been challenging, due to the fact that this habitat is characterized by the presence of understory bamboo, which is masked by the overstory deciduous and/or coniferous forest canopies (Liu et al., 2001;

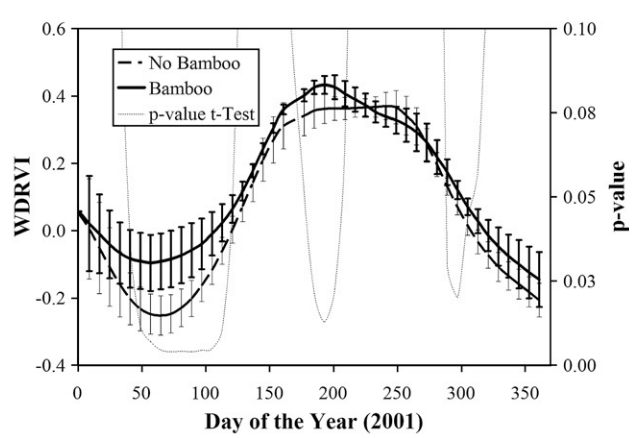


Fig. 8. Seasonal MODIS-WDRVI variation in 2001 of broadleaf deciduous forest stands with similar elevation (2200–2600 m), slope (<30°) and forest cover (>60%), but with (8 non-contiguous pixels) and without (11 non-contiguous pixels) understory umbrella bamboo (*Fargesia robusta*). *p*-values correspond to a two-sample *t*-test, after checking variance homogeneity. Error bars correspond to 2 SEM.

Linderman et al., 2004, 2005). Therefore, analyses of panda habitat using remote sensing techniques should incorporate other perspectives in addition to the spectral characterization. In this study, the underlying hypothesis was that the phenological progression of the vegetation constitutes a suitable environmental predictor for giant panda habitat mapping, as it could characterize the panda habitat in the temporal domain (in addition to the spectral domain provided by single-date multi-spectral imagery). To further support this hypothesis, we obtained the phenological curves of 19 non-contiguous MODIS pixels under broadleaf deciduous forest stands, with similar elevation (2200–2600 m), slope (<30°) and canopy cover (>60%), but with (>70% cover) and without (0% cover) understory bamboo (*F. robusta*). On average, the broadleaf deciduous pixels with understory bamboo have 15.8% higher WDRVI values than those without understory bamboo (Fig. 8). In addition, these stands are significantly different (i.e., $p$-value $<0.05$; two-sample $t$-test, after checking variance homogeneity) at three time periods: 1) February 10 to April 30; 2) July 4 to July 28; and 3) October 16 to November 9 (Fig. 8). These differences in total canopy green biomass (as measured by WDRVI), as well as the asynchronous phenologies between forests with and without understory bamboo support our logic for using high temporal resolution MODIS data for panda habitat characterization.

Nevertheless, there is a compromise between temporal and spatial resolutions, since the data acquired with high temporal resolution is also acquired with coarser spatial resolutions (AVHRR, MODIS). Therefore, issues of spatial resolution must be addressed. In general terms, when the scale of measurement of a variable changes, the variance of that variable also changes, but the magnitude and type of this change depends on the complexity of the area under study (Wiens, 1989). The spatial complexity is dependent upon the number of separable land surface units present within it, as well as their size and spatial arrangement. Thus, the degree of heterogeneity that a sensor system can detect is a function of both the complexity of the landscape studied and the spatial resolution of the sensor system (Woodcock & Strahler, 1987; Cao & Lam, 1997).

Since the study area has a high complexity due mostly to drastic changes in topography, more variance is contained within a single pixel of the MODIS sensor. Thus, deciding if a particular pixel constitutes panda habitat under a binary decision rule (habitat vs. non-habitat) is difficult and potentially biased. Therefore, for coarse spatial resolution data, a fuzzy classification algorithm based on ecological niche theory was preferred. The habitat modeling algorithm selected (ENFA) is based on species occurrence data (i.e., presence-only), therefore a formal comparison of the results obtained using different models and remotely sensed datasets is difficult, due to the lack of confirmed absences. Nonetheless, a validation procedure specifically designed for presence-only data showed that the ENFA model, using a coarse spatial resolution MODIS-WDRVI time series dataset, provided a similar prediction success as well as similar areal estimates of total panda habitat to those obtained by the single-date, 30 m/pixel Landsat TM dataset used with a DEM in the four-category scheme modeling procedure. This further confirms that the seasonal variability of the vegetation provides suitable information for separating (among the enormous variability of conditions that characterize the panda habitat) forests that constitute giant panda habitat from those that do not. Therefore, datasets that characterize the spatio-temporal variability of vegetation are also carriers of information to be used for giant panda habitat mapping. In addition, since only the spatio-temporal variability of vegetation was used, it also shows that vegetation is an efficient integrator of topographic, geographic, and climatic conditions (Peters et al., 2002). This capability, in combination with the extensive areal coverage of MODIS data, will aid in the generation of management practices and conservation decisions that cover the entire panda population in its entire geographic range, as opposed to the localized analyses that have been applied at the level of nature reserves (Liu et al., 2001, 2004; Viña et al., 2007).

The approaches used in the present study could be applied for the analyses of the habitat of many other wildlife species in large geographic extents, as well as for establishing management strategies that require a view of their entire geographic ranges. The design and implementation of conservation policies that enhance the connectivity among areas of suitable habitat for threatened or endangered wildlife species, as well as establish buffer areas to mitigate the influence of human activities, will benefit from the perspective given by analyzing the entire geographic range of the species of interest. Thus, this approach offers new insights for biodiversity conservation.

## Acknowledgements

We thank the Administration of Wolong Nature Reserve for their support with fieldwork logistics and particularly recognize the assistance from Jinyan Huang, Mingchong Liu, Yinchun Tan, Jian Yang, and Shiqiang Zhou. Omnistar, Singapore provided satellite signal for the differential correction of our global positioning system receivers during field data campaigns. William McConnell, Wei Liu and two anonymous reviewers provided important suggestions to the manuscript. We gratefully acknowledge the financial support from the National Science Foundation (Dynamics of Coupled Natural and Human Systems program), the National Institutes of Health (National Institute of Child Health and Human Development, R01 HD39789), the National Aeronautics and Space Administration (Land Use/Land Cover Change program and Terrestrial Ecology and Biodiversity program), the National Natural Science Foundation of China (30428028), and the Chinese Academy of Sciences, Ministry of Science and Technology of China (G2000046807).

## References

Asrar, G., Myneni, R. B., & Choudhury, B. J. (1992). Spatial heterogeneity in vegetation canopies and remote sensing of absorbed photosynthetically active radiation: A modeling study. *Remote Sensing of Environment*, *41*, 85−103.

Bearer, S.L., (2005), The effects of forest harvesting on giant panda habitat use in Wolong Nature Reserve, China. Ph. D. Dissertation. Michigan State University.

Borel, C. C., & Gerstl, S. A. W. (1994). Nonlinear spectral mixing models for vegetative and soil surfaces. *Remote Sensing of Environment*, *47*, 403−416.

Boyce, M. S., Vernier, P. R., Nielsen, S. E., & Schmiegelow, F. K. A. (2002). Evaluating resource selection functions. *Ecological Modelling*, *157*, 281−300.

Cao, C., & Lam, N. S. (1997). Understanding the scale and resolution effects in remote sensing and GIS. In M. F. Goodchild (Ed.), *Scale in remote sensing and GIS* (pp. 57−72). Lewis Publishers.

Engler, R., Guisan, A., & Rechsteiner, L. (2004). An improved approach for predicting the distribution of rare and endangered species from occurrence and pseudo-absence data. *Journal of Applied Ecology*, *41*, 263−274.

Fielding, A. L., & Bell, J. F. (1997). A review of methods for the assessment of prediction errors in conservation presence/absence models. *Environmental Conservation*, *24*, 38−49.

Gardner, R. H., Milne, B. T., Turner, M. G., & O'Neill, R. V. (1987). Neutral models for the analysis of broad-scale landscape patterns. *Landscape Ecology*, *1*, 19−28.

Gitelson, A. A. (2004). Wide Dynamic Range Vegetation Index for remote quantification of biophysical characteristics of vegetation. *Journal of Plant Physiology*, *161*, 165−173.

Gitelson, A. A., Viña, A., Arkebauer, T. J., Rundquist, D. C., Keydan, G., & Leavitt, B. (2003). Remote estimation of leaf area index and green leaf biomass in maize canopies. *Geophysical Research Letters*, *30*, 1248. doi:10.1029/2002GL016450

Gitelson, A. A., Viña, A., Ciganda, V., Rundquist, D. C., & Arkebauer, T. J. (2005). Remote estimation of canopy chlorophyll content in crops. *Geophysical Research Letters*, *32*, L08403. doi:10.1029/2005GL022688

Goward, S. M., & Huemmerich, K. E. (1992). Vegetation canopy PAR absorptance and the Normalized Difference Vegetation Index: An assessment using SAIL model. *Remote Sensing of Environment*, *39*, 119−140.

He, N., Liang, C., & Yin, X. (1996). Sustainable community development in Wolong Nature Reserve. *Ecological Economy*, *1*, 15−23.

Henebry, G. M., Viña, A., & Gitelson, A. A. (2004). The Wide Dynamic Range Vegetation Index and its potential utility for gap analysis. *GAP Analysis Program Bulletin*, *12*, 50−56.

Hirzel, A. H., & Arlettaz, R. (2003). Modeling habitat suitability for complex species distributions by environmental-distance geometric mean. *Environmental Management*, *32*, 614−623.

Hirzel, A. H., Hausser, J., Chessel, D., & Perrin, N. (2002). Ecological-niche factor analysis: How to compute habitat-suitability maps without absence data? *Ecology*, *83*, 2027−2036.

Hirzel, A. H., Hausser, J., & Perrin, N. (2004). *Biomapper 3.0*. Division of Conservation Biology, University of Bern URL: http://www.unil.ch/biomapper. (last date accessed: 15 September 2006).

Huete, A. R., Liu, Q., Batchily, K., & van Leeuwen, W. (1997). A comparison of vegetation indices over a global set of TM images for EOS-MODIS. *Remote Sensing of Environment*, *59*, 440−451.

Hutchinson, G. E. (1957). Concluding remarks. *Cold Spring Harbor Symposia on Quantitative Biology*, *22*, 415−427.

Jensen, J. R. (1996). *Introductory digital image processing, a remote sensing perspective*. Second edition. New Jersey: Prentice Hall.

Johnson, K., Schaller, G. B., & Hu, J. (1988). Responses of giant panda to a bamboo die-off. *National Geographic Research*, *4*, 161−177.

Li, D., Song, Y., & Ouyang, Z. (2003). *Research on the national forestry nature reserve system plan – GEF China nature reserve management project.* Beijing: China Land Press.

Linderman, M., Liu, J., Qi, J., An, L., Ouyang, Z., Yang, J., et al. (2004). Using artificial neural networks to map the spatial distribution of understory bamboo from remote sensing data. *International Journal of Remote Sensing*, *25*, 1695−1700.

Linderman, M., Bearer, S., An, L., Tan, Y. C., Ouyang, Z., & Liu, J. (2005). The effects of understory bamboo on broad-scale estimates of giant panda habitat. *Biological Conservation*, *121*, 383−390.

Liu, J., Ouyang, Z., Taylor, W. W., Groop, R., Tan, Y., & Zhang, H. (1999). A framework for evaluating the effects of human factors on wildlife habitats: The case of giant pandas. *Conservation Biology*, *13*, 1360−1370.

Liu, J., Linderman, M., Ouyang, Z., An, L., Yang, J., & Zhang, H. (2001). Ecological degradation in protected areas: The case of Wolong Nature Reserve for giant pandas. *Science*, *292*, 98−101.

Liu, X., Bronsveld, M. C., Skidmore, A. K., Wang, T., Dang, G., & Yong, Y. (2004). Mapping habitat suitability for giant pandas in Foping Nature Reserve, China. In D. Lindburg, & K. Baragona (Eds.), *Giant pandas biology and conservation* (pp. 176−186). University of California Press.

Loucks, C. J., Lü, Z., Dinerstein, E., Wang, H., Olson, D. M., Zhu, C., et al. (2001). Giant pandas in a changing landscape. *Science*, *294*, 1465.

Loucks, C. J., Lü, Z., Dinerstein, E., Wang, D., Fu, D., & Wang, H. (2003). The giant pandas of the Qinling mountains, China: A case study in designing conservation landscapes for elevational migrants. *Conservation Biology*, *17*, 558−565.

Luoto, M., Kuussaari, M., & Toivonen, T. (2002). Modelling butterfly distribution based on remote sensing data. *Journal of Biogeography*, *29*, 1027−1037.

Luoto, M., Toivonen, T., & Heikkinen, R. K. (2002). Prediction of total and rare plant species richness in agricultural landscapes from satellite images and topographic data. *Landscape Ecology*, *17*, 195−217.

MacKinnon, J., & De Wulf, R. (1994). Designing protected areas for giant pandas. In R. Miller (Ed.), *Mapping the diversity of nature* (pp. 127−142). London: Chapman & Hall.

Markham, B.L., & Barker, J.L., (1986), Landsat MSS and TM post-calibration dynamic ranges, exoatmospheric reflectances and at-satellite temperatures. *EOSAT technical notes*, No. 1, August.

Morisette, J. T., Jarnevich, C. S., Ullah, A., Cai, W., Pedelty, J. A., Gentle, J. E., et al. (2006). A tamarisk habitat suitability map for the continental United States. *Frontiers in Ecology and the Environment*, *4*, 11−17.

Myneni, R. B., Nemani, R. R., & Running, S. W. (1997). Estimation of global leaf area and absorbed PAR using radiative transfer models. *IEEE Transaction on Geoscience and Remote Sensing*, *35*, 1380−1393.

Nielsen, S. E., Boyce, M. S., Stenhouse, G. B., & Munro, R. H. M. (2003). Development and testing of phenologically driven grizzly bear habitat models. *Ecoscience*, *10*, 1−10.

Ouyang, Z., Zhang, H., Tan, Y., Zhang, K., Li, H., & Zhou, S. (1995). Application of GIS in evaluating giant panda habitat in Wolong Nature Reserve. *China's Biosphere Reserve*, *3*, 13−18.

Pan, W., Lü, Z., Wang, D., & Wang, H. (2001). The opportunity for the giant panda to exist. Beijing: Peking University Press.

Perrin, N., (1984), Contribution à l'écologie du genre Cepaea (Gastropoda): Approche descriptive et expérimentale de l'habitat et de la niche écologique. Ph. D. Dissertation. Institut de Zoologie et d'Ecologie Animale. Lausanne, Switzerland.

Peters, A. J., Walter-Shea, E. A., Ji, L., Viña, A., Hayes, M., & Svoboda, M. D. (2002). Drought monitoring with NDVI-based Standardized Vegetation Index. *Photogrammetric Engineering and Remote Sensing*, *68*, 71−75.

Peterson, E. B. (2005). Estimating cover of an invasive grass (*Bromus tectorum*) using tobit regression and phenology derived from two dates of Landsat ETM+ data. *International Journal of Remote Sensing*, *26*, 2491−2507.

Reid, D. G., & Hu, J. (1991). Giant panda selection between *Bashania fangiana* bamboo habitats in Wolong Reserve, Sichuan China. *Journal of Applied Ecology*, *28*, 228−243.

Reid, D. G., & Gong, J. (1999). Giant panda conservation action plan. In C. Servheen, S. Herrero, & B. Peyton (Eds.), *Bears: Status survey and conservation action plan* (pp. 241−254). Gland, Switzerland: IUCN.

Reid, D. G., Hu, J. C., Sai, D., Wei, W., & Huang, Y. (1989). Giant panda (*Ailuropoda-melanoleuca*) behavior and carrying-capacity following a bamboo die-off. *Biological Conservation*, *49*, 85−104.

Reid, D. G., Taylor, A. H., Hu, J. C., & Qin, Z. S. (1991). Environmental influences on bamboo Bashania fangiana growth and implications for giant panda conservation. *Journal of Applied Ecology*, *28*, 855−868.

Roerink, J. G., Menenti, M., & Verhoef, W. (2000). Reconstructing cloud-free NDVI composites using Fourier analysis of time series. *International Journal of Remote Sensing*, *21*, 1911−1917.

Rouse, J. W., Haas, R. H., Jr., Schell, J. A., & Deering, D. W. (1974). Monitoring vegetation systems in the Great Plains with ERTS. *Third ERTS-1 Symposium*, *vol. 1*. (pp. 309−317)Washington, D.C.: NASA SP-351.

Rushton, S. P., Ormerod, S. J., & Kerby, G. (2004). New paradigms for modeling species distributions? *Journal of Applied Ecology*, *41*, 193−200.

Schaller, G. B., Hu, J., Pan, W., & Zhu, J. (1985). The giant pandas of Wolong Chicago, Illinois: University of Chicago Press.

Sellers, P. J. (1985). Canopy reflectance, photosynthesis and transpiration. *International Journal of Remote Sensing*, *6*, 1335−1372.

Seto, K. C., Fleishman, E., Fay, J. P., & Betrus, C. J. (2004). Linking spatial patterns of bird and butterfly species richness with Landsat TM derived NDVI. *International Journal of Remote Sensing*, *25*, 4309−4324.

Taylor, A. H., & Qin, Z. (1987). Culm dynamics and dry matter production of bamboos in the Wolong and Tangjiahe giant panda reserves Sichuan, China. *Journal of Applied Ecology*, *24*, 419−434.

Taylor, A. H., & Qin, Z. (1993). Bamboo regeneration after flowering in the Wolong Giant Panda Reserve, China. *Biological Conservation*, *63*, 231−234.

Verhoef, W., Menenti, M., & Azzall, S. (1996). A color composite of NOAA-AVHRR based on time series (1981–1992). *International Journal of Remote Sensing*, *17*, 231−235.

Viña, A., Henebry, G. M., & Gitelson, A. A. (2004). Satellite monitoring of vegetation dynamics: Sensitivity enhancement by the Wide Dynamic Range Vegetation Index. *Geophysical Research Letters*, *31*, L04503. doi:10.1029/2003GL019034

Viña, A., & Gitelson, A. A. (2005). New developments in the remote estimation of the fraction of absorbed photosynthetically active radiation in crops. *Geophysical Research Letters*, *32*, L17403. doi:10.1029/2005GL023647

Viña, A., Bearer, S., Chen, X., He, G., Linderman, M., An, L., et al. (2007). Temporal changes of giant panda habitat connectivity across boundaries of Wolong Nature Reserve, China. *Ecological Applications*, *17*, 1019−1030.

Wei, F., Zhang, Z., & Zhang, Z. (2006). History, current situation and future of in-situ and ex-situ conservation of the giant panda. In Z. Zhang, & F. Wei (Eds.), *Giant panda ex-situ conservation theory and practice* (pp. 13−54). Beijing, China: Science Publishing House.

Wiens, J. A. (1989). Spatial scaling in ecology. *Functional Ecology*, *3*, 385−397.

Woodcock, C. E., & Strahler, A. H. (1987). The factor of scale in remote-sensing. *Remote Sensing of Environment*, *21*, 311−332.

Xu, W., Ouyang, Z., Viña, A., Zheng, H., Liu, J., & Xiao, Y. (2006). Designing a conservation plan for protecting the habitat for the giant pandas in the Qionglai mountain range, China. *Diversity and Distributions*, *12*, 610−619.

Yan, X. (2005). Status, challenge and prospect of wild giant pandas. *Acta Theriologica Sinica*, *25*, 402−406.

Zhang, H., Li, D., Wei, R., Tang, C., & Tu, J. (1997). Advances in conservation and studies on reproductivity of giant pandas in Wolong. *Sichuan Journal of Zoology*, *16*, 31−33.